

pubs.acs.org/journal/ascecg Research Article

Acidic Ethanol/Water Casting Approach to Improve Chitin Nanofibril Dispersion and Properties of Propionylated Chitin Biocomposites

Tuhua Zhong,* Michael P. Wolcott, Hang Liu, and Jinwu Wang*



Cite This: ACS Sustainable Chem. Eng. 2021, 9, 3289-3299

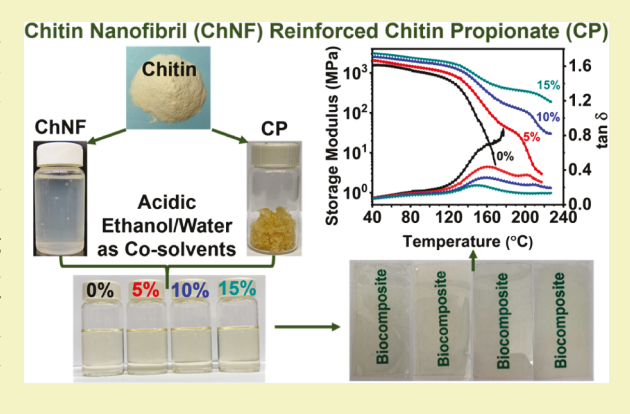


ACCESS

Metrics & More

Article Recommendations

ABSTRACT: A fabrication process using acidic ethanol/water as a medium was developed to achieve homogenous dispersion of chitin nanofibrils (ChNFs) in a chitin propionate (CP) solution to form ChNF-reinforced CP nanocomposites. CP was prepared by propionylation of chitin to improve its dissolution in green organic solvents. ChNFs were extracted from chitin via partial alkali deacetylation in water. An acidified ethanol/water mixture as a medium was found to dissolve CP and disperse ChNF suspensions simultaneously, forming clear and stable formulations. The degree of ChNF dispersion and compatibility between ChNF and CP in the acidified ethanol/water mixture yielded transparent ChNF-reinforced CP nanocomposites with a moderate UV-blocking capability of up to 76%. The tensile strength and modulus of 15% ChNF-filled nanocomposites were enhanced by 66 and 97%, respectively, when compared to the neat films. In addition, the



maximum degradation temperature was increased by 40 °C. The increase in storage modulus was more pronounced above the glass transition temperature. These results demonstrated that ChNFs had substantial reinforcing effects on the cast CP nanocomposites. **KEYWORDS:** chitin propionate, chitin nanofibrils, non-toxic solvents, bio-nano composites, mechanical performance, thermal stability

■ INTRODUCTION

There is a growing interest in using biomass as a source of renewable materials. Chitin is the second most abundant biopolymer on earth but is still underutilized. Chitin cannot dissolve in water and most common organic solvents as a result of its supramolecular structure; it is difficult to process chitin for practical applications. Some aggressive solvents, for example, dimethylacetamide/lithium chloride (DMAc/LiCl) or ionic liquids, can dissolve chitin but are toxic or expensive, so they are impractical for industry applications. To overcome the poor solubility of chitin, chemical modification is often needed.

Esterification and acylation are the most common approaches to be successfully applied in modifying polysaccharides like cellulose and chitin, especially for cellulose. Through the conventional esterification or acylation approach, cellulose derivatives, for example, cellulose acetate, cellulose propionate, and cellulose acetate butyrate, have been commercially available. Esterification or acylation of cellulose by introducing hydrophobic acyloxy groups bearing longer carbon chains to replace hydroxy groups can increase its solubility in most common organic solvents (e.g., alcohol, ethyl acetate, etc.). The solubility of cellulose esters or cellulose acylates in most common organic solvents has opened the door for their uses in a wide variety of fields such as coatings, resins,

composites, optical films, membranes, and so forth. Chitin was structurally similar to cellulose; the minor difference is that the acetamido group instead of the hydroxyl group exists at the C2 position in the anhydro-glucosamine unit. Due to the structural similarity between chitin and cellulose, well-developed esterification or acylation approaches for cellulose may be used to chemically modify chitin, thereby enhancing its solubility in organic solvents.

Conventional acylation is an effective method of modifying polysaccharides cellulose and chitin. The acylation reaction of chitin may occur under a homogeneous condition or a heterogeneous condition. The former often requires the dissolution of chitin in DMAc/Li or ionic liquids to form a homogeneous solution before derivatization. The latter does not require additional organic solvents, but it often requires excessive acid anhydride as an acylation agent and dispersion reagent in the presence of a mineral acid as a catalyst for the derivatization of chitin. ¹¹ Compared to strong organic solvents

Received: December 10, 2020 Revised: January 13, 2021 Published: February 16, 2021





(e.g., DMAc/LiCl) or ionic liquids (e.g., 1-allyl-3-methylimidazolium bromide), the use of acid anhydrides such as acetate anhydride and propionate anhydride is relatively much cheaper or more cost effective, although excessive acid anhydride is often required to ensure well dispersion and full acylation of chitin during the reaction. The commercial production of cellulose acetate and cellulose propionate adopts a wellestablished heterogeneous reaction. However, the acylation approach usually results in severe polymer degradation and the breakdown of the original crystalline structures, which inevitably deteriorates material properties when compared to their raw materials. This effect is especially prevalent for thermal stability; as noted above, the acylation process often involves harsh reaction conditions with corrosive chemicals such as sulfuric acid or perchloric acid as a catalyst. 12 To improve the material properties of cellulose- or chitin-based esters, nanoreinforcement is often used because nanoreinforcing materials can provide improvements in stiffness, strength, toughness, thermal stability, and barrier performance. 13 Among the nanoreinforcements, naturally produced polysaccharide nanofibrils are more attractive because they are renewable, nontoxic, biodegradable, and biocompatible.14 Similar to cellulose microfibrils in the plant cell wall, chitin microfibrils serve as a fundamental reinforcing constituent within the shell structure of crabs, lobsters, and shrimps. 15 Biological chitin microfibrils can be isolated into a technical product of chitin nanofibrils (ChNFs).

ChNF extraction usually demands chemical- or mechanical pretreatment followed by mechanical disintegration; common chemical pretreatments include 2,2,6,6-tetramethylpiperidine-1-oxyl radical-mediated oxidation, strong acid hydrolysis, and strong alkali hydrolysis. $^{16-18}$ Alkali hydrolysis is a traditional method to produce chitosan and a facile approach to generate positively charged surfaces in chitin. Treatment conditions such as temperature, time, and alkali concentration can be tuned to control the degree of deacetylation to prevent the severe degradation of the crystalline structure. 18 After partial alkali deacetylation, acetamido groups in chitin molecules can be converted into amine groups, which were further protonated under mild acidic conditions to form ammonium cations (NH₃⁺) on chitin fibril surfaces. ¹⁸ Positively charged surfaces can facilitate the liberation of the nanofibrils and can promote stable dispersion of ChNF in acidic water because of interfibrillar electrostatic repulsion forces. ChNFs often render excellent material properties such as high specific surface areas, high strength and modulus, low density, and low coefficient of thermal expansion, which make ChNF an ideal reinforcing material for polymer composites. 14,15

Water is a common medium used extensively in ChNF extraction processing. However, as with cellulose nanofibrils (CNFs), the removal of water from ChNF suspensions is known to cause agglomeration and aggregation of the nanofibrils. When applied as a reinforcement in polymeric matrices, water-based ChNF suspensions are preferably blended with water-soluble polymers or polymer aqueous dispersions (lattices) because water removal from the ChNF suspension can be avoided and the dispersed state of the nanofibrils can be preserved in this mode. Help 14,20,21 When a solvent is required for the dissolution of polymeric matrices, the polysaccharide nanofibrils must undergo solvent exchange or an initial freeze or spray drying process, re-dispersed and finally mixed with polymer solutions. As mentioned previously, aggregation might be inevitable upon drying,

imparting poor dispersion when blending dried aggregated nanofibrils with melting polymers. ^{14,22,23} The direct use of ChNFs in water with other polymers in organic solvents could avoid the water removal step that often involves a freeze and spray drying or solvent exchange process, which may help reduce the energy input or avoid additional solvent usage.

An efficient and effective processing technique is crucial to ensure the improved material properties of the resulting nanocomposites. It remains challenging to homogeneously blend hydrophilic polysaccharide-based nanofibrils with hydrophobic polymers. The present work is aimed at developing an effective and efficient method to directly mix ChNFs in water with a chitin derivative chitin propionate (CP) in organic solvents to form well-dispersed nanocomposite formulations to produce highly transparent ChNF-reinforced CP nanocomposites. CP as the matrix was prepared by the propionylation process to improve its solubility in organic solvents, and partially deacetylated ChNFs were prepared to be used as the reinforcement. Acidified ethanol/water mixtures were used as a medium to dissolve CP and disperse ChNF simultaneously to form stable CP/ChNF suspensions with varying ChNF concentrations for casting. The mechanical and thermal properties of the resulting nanocomposites were measured, and the ChNF reinforcing effects in the CP matrix were examined.

■ EXPERIMENTAL SECTION

Materials. Chitin from shrimp shells (powder, practical grade), propionic anhydride (97%), perchloric acid (ACS reagent, 70%), and sodium borohydride were from Sigma Aldrich. Ethanol (200 proof, anhydrous) was from Decon Labs, Inc. Glyceryl triacetate used as a plasticizer was kindly provided by Siegwerk USA Co. Glacial acetic acid (ACS reagent) was from EMD Millipore Corporation.

CP Preparation. CP was manufactured following our previously developed procedures. 24 Briefly, chitin powder (20 g) was treated by propionic anhydride (132 g) with perchloric acid (10 g) as a catalyst at 0 °C for 0.5 h and then at 20 °C for 2.5 h. Upon the defined reaction time, unreacted propionic anhydride was hydrolyzed by adding diluted acetic acid solution and then five-fold water. Waterinsoluble CP precipitated in water and was then collected by filtration and washing until the pH was neutral and finally was dried at 70 °C in an oven overnight. CP powder dissolved in 90% aqueous ethanol solution (ethanol/water: 90/10, % w/w), and the insoluble parts were removed by centrifugation at 9000 rpm. The soluble CP solution was subject to rotary evaporation to remove the solvents and then was airdried for several days to obtain the solid CP.

ChNF Extraction. Chitin (4 g) was suspended in 33 wt % sodium hydroxide solution (100 mL) containing sodium borohydride (0.12 g). The mixture was autoclaved at 121 °C in a lab autoclave (Sanyo, Japan) for 3 h. After autoclaving, the mixture was washed by centrifugation at 9000 rpm for 10 min three times and then followed by dialysis against water for three days to remove chemical residuals. The partially deacetylated chitin suspension was adjusted to a concentration of 1 wt % by water and a pH of 3 by acetic acid and then was passed through an LM20 Microfluidizer (Microfluidics, USA) at a pressure of 30000 psi to obtain a transparent ChNF gel.

CP/ChNF Nanocomposite Fabrication. A series of CP/ChNF nanocomposites with different ChNF contents were fabricated according to the composition presented in Table 1 ("parts" refers to "mass"). Briefly, the predefined grams of ChNF dispersion (0.6 wt %) were added to glass vials containing the solid CP, and then, the predefined amounts of ethanol, water, plasticizer, and acetic acid were added. The mixture was ultrasonicated for 10 min to disperse ChNF well and dissolve CP. The dispersion was cast onto a leveled silicon mold (55 mm × 25 mm) to form a nanocomposite. The nanocomposites were dried overnight at room temperature at an ambient environment for 48 h and then peeled off the mold. Based on

Table 1. Composition for the Fabrication of CP/ChNF Nanocomposites

	samples			
components	CP/ChNF0	CP/ChNF5	CP/ChNF10	CP/ChNF15
CP (parts)	1.0	1.0	1.0	1.0
ChNF dispersion (0.6 wt %) (parts)	0	8.3	16.7	25
ethanol (parts)	66.3	66.3	66.3	58.0
water (parts)	16.6	8.3	0	0
acetic acid (parts)	4.1	4.1	4.1	4.1
plasticizer (parts)	0.6	0.6	0.6	0.6

the ChNF loadings of 0, 5, 10, and 15%, the samples were labeled as CP/ChNF0, CP/ChNF5, CP/ChNF10, and CP/ChNF15, respectively.

Characterizations. The liquid-state 1 H nuclear magnetic resonance (NMR) spectrum of CP in deuterated dimethyl sulfoxide (DMSO- d_{6}) was measured with a Varian 400-NMR spectrometer (400 Hz, Bruker, USA) at 32 scans in the chemical shift range of 0–12 ppm. The degree of substitution of propionyl groups (DS_{pr}) was calculated using the formula 1 described by Teramoto et al.

$$DS_{pr} = \frac{7I_{CH_3}}{3I_{H1-6}} \tag{1}$$

where $I_{\rm CH_3}$ is the integral area of the methyl proton signal of propionyl groups and $I_{\rm H1-6}$ is the integral area of the 7-proton signal in an anhydro-glucosamine unit.

The Fourier-transform infrared (FTIR) spectra of chitin and ChNFs were recorded in an absorbance mode by a Nicolet iS-50 FTIR spectrometer (Thermo Fisher Scientific, USA) at a 4 cm $^{-1}$ resolution and 64 scans in the range from 4000 to 400 cm $^{-1}$. Before FTIR analysis, the thin pellets consisting of the samples and potassium bromide (1/50, % w/w) were prepared. The degree of acetylation of the partially deacetylated ChNFs was estimated with the eq 2 proposed by Brugnerotto et al. $^{2.5}$

$$DA \% = 31.92 \times A_{1320} / A_{1420} - 12.20$$
 (2)

$$DDA \% = 100 - DA \%$$
 (3)

where DA is the degree of acetylation of ChNFs and DDA is the degree of deacetylation; the A_{1320}/A_{1420} ratio is the absorption ratio at the bands 1320 and 1420 cm⁻¹, and the intensities of the IR absorption band maxima at 1320 and 1420 cm⁻¹ were determined according to the baseline method. ^{25,26}

The zeta potential of partially deacetylated ChNFs in water (concentration: 0.02 wt %, pH = 3) was measured with a Nano-Zetasizer (Malvern Instruments, UK) at 20 $^{\circ}$ C.

The ChNF morphology was observed with Tecnai G2 20 Twin transmission electron microscopy (TEM, FEI, USA) operating at 200 kV. Diluted ChNF dispersion was deposited onto a Formvar/carbon-coated copper grid and then was stained by 2% uranyl acetate and finally was dried overnight before TEM analysis.

The diffractograms of chitin, CP, and the nanocomposites were measured using a Miniflex 600 X-ray diffractometer (Rigaku, Japan) with a Cu K α X-ray source (λ = 0.1548 nm) at 40 kV and 15 mA. The crystallinity index (CrI) was calculated using the formula 4. ¹⁷

$$CrI = \frac{(I_{110} - I_{amorphous})}{I_{110}} \times 100\%$$
 (4)

where I_{110} is peak (110) intensity and $I_{\rm amorphous}$ is the baseline intensity at $2\theta=16.0^{\circ}$.

The microstructure of the nanocomposites with different ChNF contents was observed with Quanta 200F scanning electron microscopy (SEM, FEI, USA) at 20 kV. Before SEM observation, all the samples were cryofractured and then were coated with platinum via a sputter.

The light transmittance of the nanocomposites was recorded with a Lambda-25 UV—vis spectrophotometer (PerkinElmer, USA) at a wavelength of 200–800 nm.

The tensile properties of the nanocomposites were tested by an Instron 4466 testing system (Instron, USA) equipped with a 100 N load cell at an initial grip separation of 2 mm and testing speed of 2 mm/min. Five specimens for each sample were measured.

The dynamical mechanical analysis was performed with a Q800 dynamic mechanical tester (TA Instruments, USA) in a tension mode under a strain amplitude of 25 μ m and preload force of 0.001 N, ramping from 30 to 230 °C at 3 °C/min.

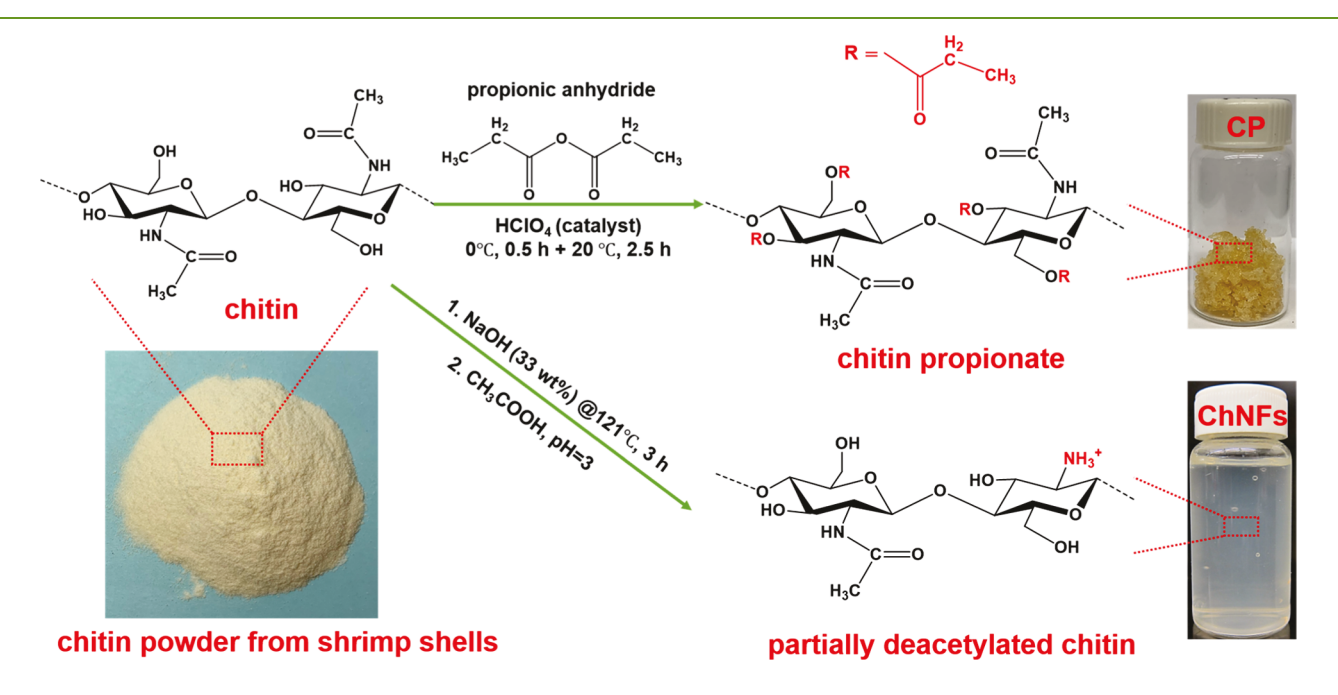


Figure 1. Scheme of chemical reaction of chitin from shrimp shells to produce CP and partially deacetylated ChNFs.

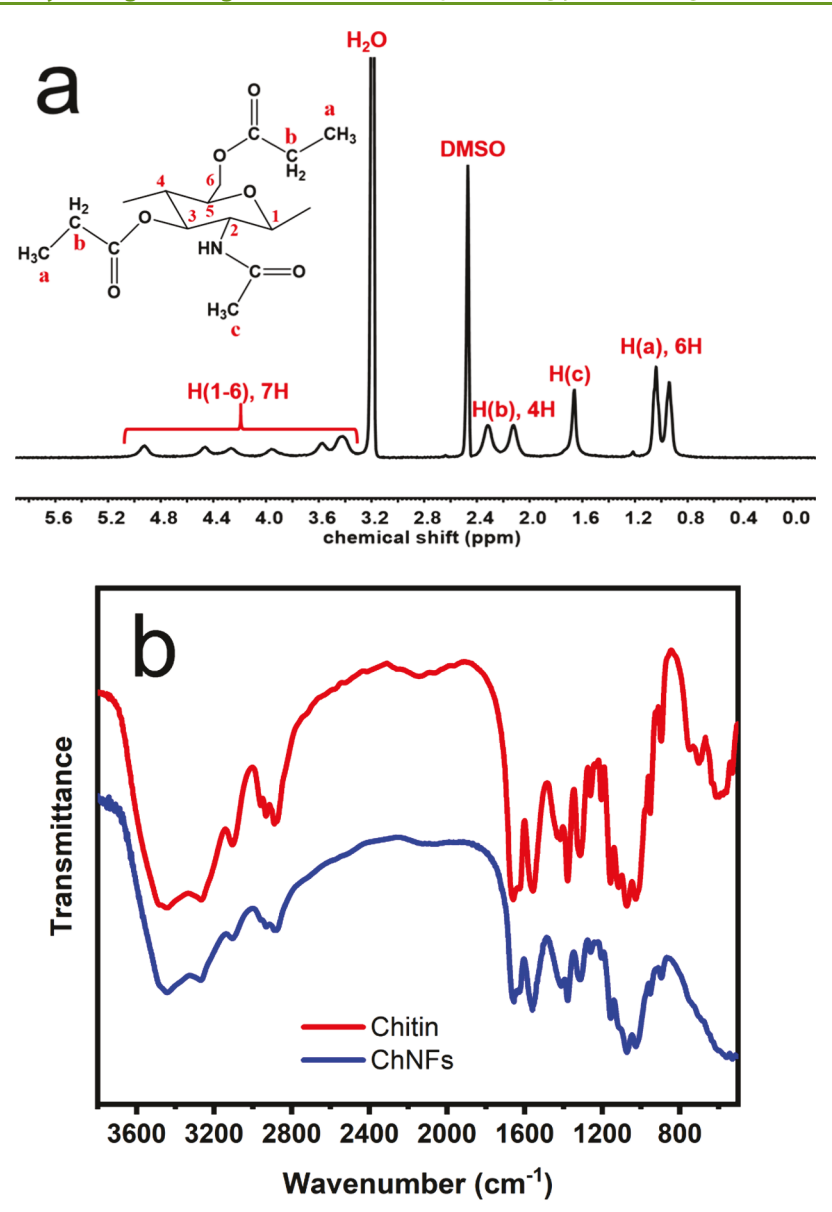


Figure 2. ¹H NMR spectrum (a) of CP in deuterated DMSO-d₆ and FTIR spectra (b) of chitin and partially deacetylated ChNFs.

The thermal stability was assessed by a STAR system thermogravimetric analyzer (Mettler Toledo, USA), ramping up from 25 to 600 °C at 10 °C/min and with purging nitrogen of 100 mL/min.

■ RESULTS AND DISCUSSION

Characteristics of CP and ChNFs. To dissolve chitin in organic solvents, chitin was first esterified under a heterogeneous process. As shown in Figure 1, chitin from shrimp shells was modified with propionic anhydride in the presence of perchloric acid as a catalyst but without other solvents. Highly propionyl-substituted chitin was obtained. The degree of substation of propionyl groups was approximately 2, which was confirmed by ¹H NMR analysis. The result was also consistent with our previous study. ²⁴ To facilitate the liberation of nanofibrils from chitin microfibrils in a mechanical disintegration device (i.e., high-pressure homogenizer), chitin was pretreated in a concentrated sodium hydroxide solution to partially convert acetamido groups (–NHCOCH₃) into amine groups (NH₂). The amine groups in the partially deacetylated

chitin were further converted into ammonium cations (-NH₃⁺) under mild acidic conditions, which induced the interfibrillar electrostatic repulsion forces, thus resulting in ease of nanofibrillation and eventually leading to the generation of transparent ChNF dispersion (Figure 1) obtained with a subsequent aid of high-pressure homogenization. Figure 2b compares the FTIR spectra of as-received chitin powder and the resulting partially deacetylated ChNFs. As for chitin, the bands at 2890 cm⁻¹ corresponded to asymmetric stretching of -CH₃ from acetamido groups in chitin molecules. One strong band was observed at 1662 cm⁻¹, which was ascribed to the stretching vibration of the C=O of the acetamido groups.^{3,27} Another strong band around 1376 cm⁻¹ was observed, which was ascribed to the overlapping of C-H bending in the ring and C-CH₃ bending.²⁷ In the spectra of the ChNFs, the intensity of these bands at 2890, 1662, and 1376 cm⁻¹ associated with the acetamido groups was reduced as a result of partial deacetylation during alkali hydrolysis. One specific band at 1320 cm⁻¹ was ascribed to N-acetylglucosamine, and the band 1420 cm⁻¹ corresponded to -CH₂ bending

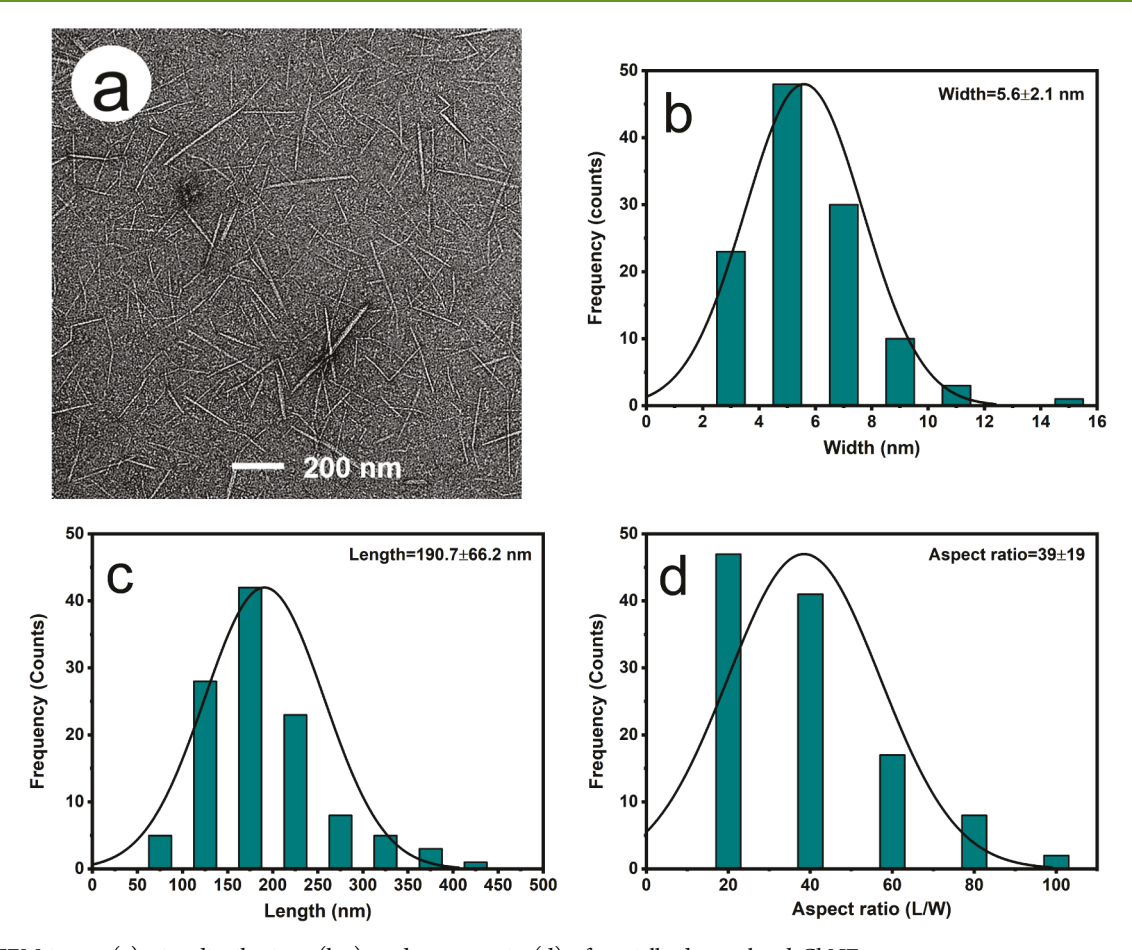


Figure 3. TEM image (a), size distributions (b,c), and aspect ratio (d) of partially deacetylated ChNFs.

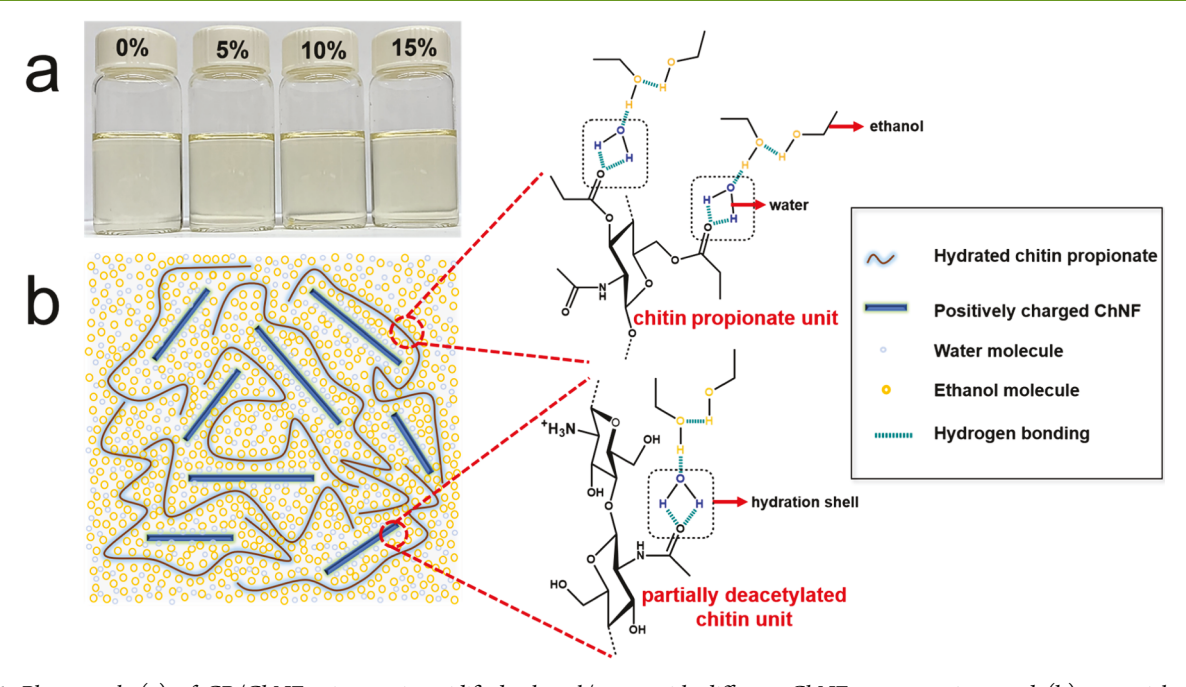


Figure 4. Photograph (a) of CP/ChNF mixtures in acidified ethanol/water with different ChNF concentrations and (b) potential molecular interaction in CP/ChNF mixtures in acidified ethanol/water.

vibration. 25,27 The A_{1320}/A_{1420} absorption ratio was often used to estimate the DA value of chitin and chitosan because the absorption ratio A_{1320}/A_{1420} showed superior agreement between the absolute and estimated DA values, regardless of

the technique, state, and secondary structure.²⁵ After partial deacetylation followed by mechanical disintegration, the DDA value of the resultant ChNFs was approximately 39% (the DA value = 61%). The zeta potential of the partially deacetylated

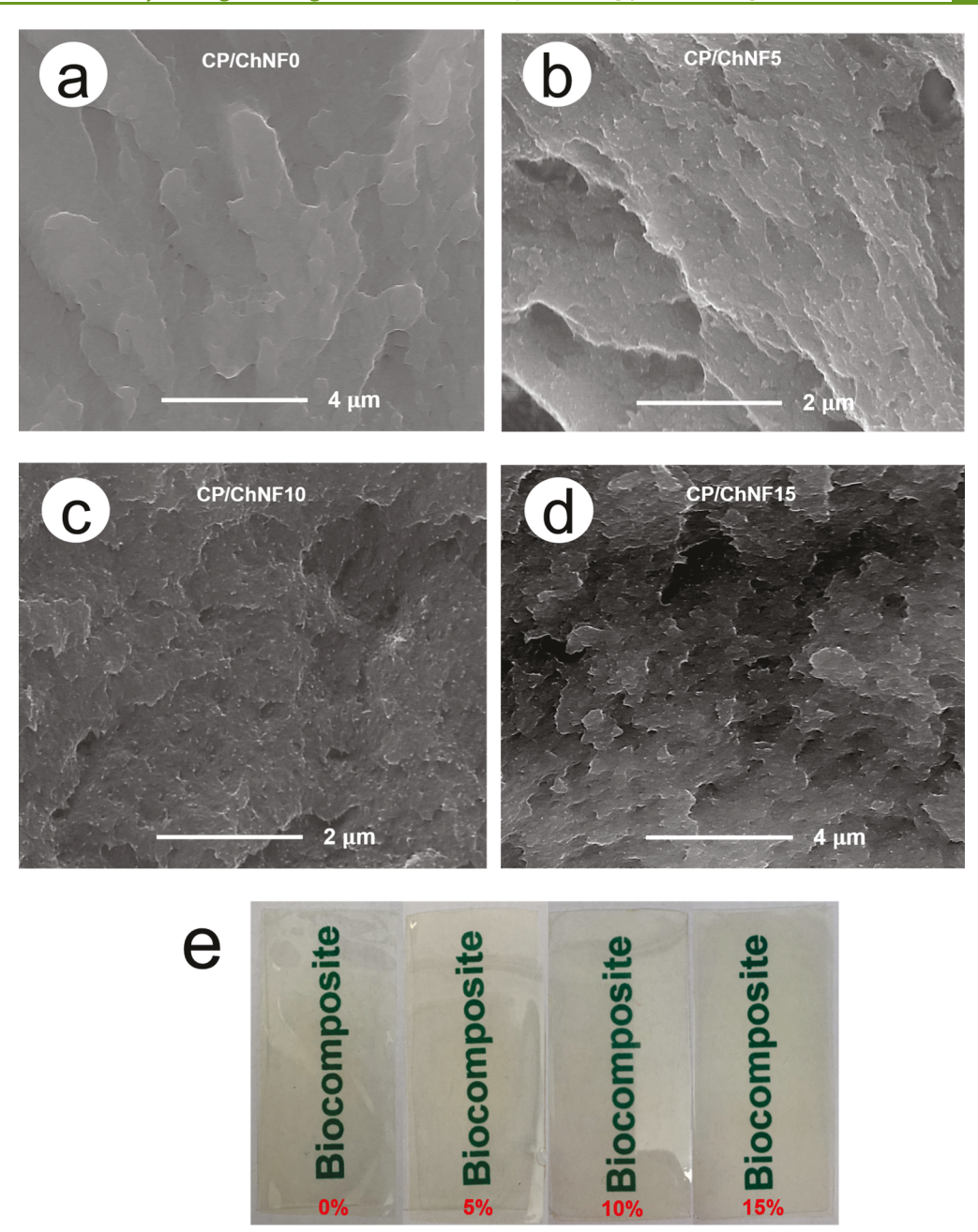


Figure 5. SEM images of the cryo-fracture microstructure of the nanocomposites (a) CP/ChNF0, (b) CP/ChNF5, (c) CP/ChNF10, and (d) CP/ChNF(15); (e) photographs of the CP/ChNF nanocomposite films with various ChNF contents (0, 5, 10, and 15%).

ChNFs was 74 ± 2 mV at a pH of 3. The high positive charge on the ChNF surface was mainly ascribed to the protonation of the amino groups ($-NH_2$) at the C2 position under the acidic condition (pH = 3), which also confirmed that partial deacetylation of chitin was achieved under the conditions used.

The needle-like morphology of ChNFs in the transparent gel in Figure 1 was observed by TEM. Figure 3a clearly shows that the partial alkali deacetylation and subsequent mechanical disintegration in the water at pH = 3 resulted in the individualization of ChNFs. The average width and length of the ChNFs were 5.6 and 190.7 nm, respectively, with an average aspect ratio of 39. Figure 3b—d exhibits the distribution of the width, length, and aspect ratio of ChNFs. The relatively narrow distributions indicated that the preparation method effectively individualized chitin fibrils, essentially eliminating long and large bundles of fibrils.

Formulation of the CP/ChNF Nanocomposite in Acidified Ethanol/Water. Figure 4a shows the clear suspensions of CP/ChNF in an acidified ethanol/water mixture, indicating the formation of well-dispersed colloidal systems. The produced CP can dissolve neither in pure water nor in pure ethanol but was soluble in a binary ethanol/water mixture. A similar phenomenon of dissolution of polymers bearing ester moieties (i.e., poly(methyl methacrylate)) in a binary ethanol/water mixture was also reported by other researchers. The formation of hydration shells around the carbonyls of polymers via hydrogen bonding and their further interactions with ethanol molecules are thought to account for the solubility maxima in binary ethanol/water mixtures. This hypothesis has been confirmed by small-angle neutron scattering (SANS) analysis reported by Hoogenboom et al. (2009); ²⁸ the SANS result indicated the presence of a single

deuterated water molecule per poly(methyl methacrylate) repeat unit. CP bearing ester groups might show a similar way of dissolution in such binary solvents, as schematically illustrated in Figure 4b. The clear nanocomposite suspensions might also indicate well dispersion of the partially deacetylated ChNFs in acidified ethanol/water mixtures and good compatibility with CP in the mixtures. The carbonyls of acetamido groups on the ChNF surface might exhibit similar interactions with water and ethanol molecules to those in CP in binary ethanol/water (Figure 4b). In addition, the cationization (-NH₃⁺) on the ChNF surface by the addition of acetic acid in the mixture induced interfibrillar electrostatic repulsion forces, thus promoting stable suspensions. Being derived from the same material chitin, the obtained CP and ChNFs had good dispersibility and compatibility in the solvent due to their similar structures and this might help to enhance the mechanical performance of the nanocomposites.

Microstructure and Optical Transparency of CP/ChNF Nanocomposites. The produced CP/ChNF nanocomposites after solvent evaporation were completely transparent to naked eyes, as evidenced in the photographs of Figure 5e, indicating that the incorporated ChNFs were small enough and welldispersed so as not to scatter light. Figure 5a-d displays the microstructure of the cryo-fractured nanocomposites. The fractured surface was relatively smooth for the CP without ChNFs and became coarser with increasing ChNF loading. There were white dots on the fractured surfaces of the ChNF containing composites, which were identified as ChNFs. The dots increased and became more evident at higher ChNF loading. Their homogeneous distribution indicated a good dispersion level of ChNFs in the CP matrix. There were no evident gaps between the filler and matrix, particularly at higher ChNF loading in the fractured surfaces, which might be attributed to good compatibility between ChNF and CP.

Figure 6 shows the light transmittance of the nanocomposites over the light wavelength ranging from 200 to

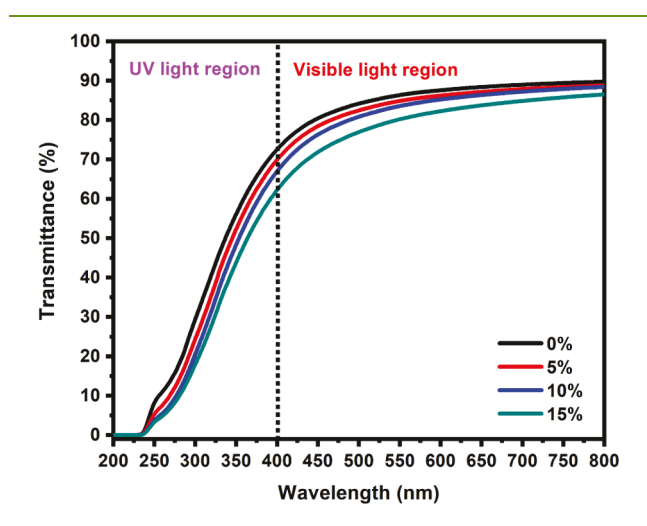


Figure 6. UV—vis spectra of the nanocomposites with various ChNF contents (0, 5, 10, and 15%).

800 nm. The light transmittance of the nanocomposites was slightly reduced with increasing ChNF content in the CP matrix. Low ChNF loading was almost not detrimental to the clarity of the CP because the particle size of ChNFs was smaller than the wavelength of visible light. ^{13,31} When ChNF loading increased to 15%, the visible light transmittance was

reduced, which might be attributed to a few agglomerations that might occur at higher ChNF loading. All the nanocomposites maintained relatively high transparency. The retained clarity of polymers with ChNF addition makes ChNF more advantageous over other nanoreinforcement materials such as carbon and clay in optical applications. The nanocomposites could block up approximately 76% of UV lights. This property is also advantageous to food packaging application in which it often demands that the packaging can block UV lights as much as possible to prevent the degradation of the packed foods; meanwhile, the retained clarity is also needed.

Physical Properties of CP/ChNF Nanocomposites. The X-ray diffraction (XRD) patterns of chitin, ChNFs, and nanocomposites are shown in Figure 7a. Chitin from shrimp shells possessed a α -type crystalline structure, as evidenced by its six characteristic peaks at $2\theta = 9.3$, 12.7, 19.3, 20.9, 23.3, and 26.4° that were ascribed to the (020), (021), (110), (120), (130), and (013) planes, respectively.³² ChNFs, prepared by partial alkali deacetylation followed by mechanical disintegration, preserved the main characteristic peaks at around 9.3 and 19.3°, indicating that the main crystalline structure was still retained, although some small characteristic peaks disappeared. The crystallinity index (CrI) of the ChNF was around 74% and was lower than that of raw chitin (CrI = 90%), which might be attributed to the partial removal of the crystalline structure as evidenced by the disappearance of the small peaks. The neat CP did not have typical peaks of the crystalline structures and became an amorphous polymer after propionylation. All the nanocomposites also displayed similar XRD patterns to the neat CP, however, with increasing ChNF loading in the CP matrix, the typical peaks of the crystalline structure of ChNF appeared more evidently in the CP nanocomposites, indicating that the crystallinity of the nanocomposites increased.

Figure 7b shows tensile strength, tensile modulus, and the elongation at break of the nanocomposites with various ChNF loadings, and Figure 7c shows the corresponding stress-strain curves. From 0 to 15% ChNF loadings in the CP matrix, there is a 66% increase in tensile strength from 26.1 to 43.4 MPa and a 97% increase in tensile modulus from 535 to 1052 MPa. It has also been reported that premixing CNFs with polylactic acid (PLA) using organic solvent acetone can retain uniform dispersion of CNFs in PLA, thus resulting in obvious enhancements in mechanical and thermomechanical properties of the CNF/PLA nanocomposites; the tensile strength and tensile modulus of the 10% CNF-filled PLA were improved by 25 and 40%, respectively.³³ It was believed that good dispersion and homogeneous distribution of ChNFs in CP in this study might largely account for the improved mechanical properties.²³ Moreover, the improvement in mechanical properties might be partly attributed to intermolecular hydrogen bonding between hydroxyl groups of ChNF and the carbonyl groups of CP because there are a large number of hydroxyl groups on the ChNF surface and carbonyl groups in CP molecules. The elongation at break was reduced with increasing ChNF loading, as shown in Figure 7b. In general, polysaccharide nanofiber/polymer composites become brittle with rigid nanofiber addition. $^{34-36}$ As discussed previously in Figure 7a, the crystallinity of the nanocomposites was enhanced with the increased ChNF loading in the CP matrix, thus leading to the increased rigidity and causing a decrease in the elongation at break of the nanocomposites.

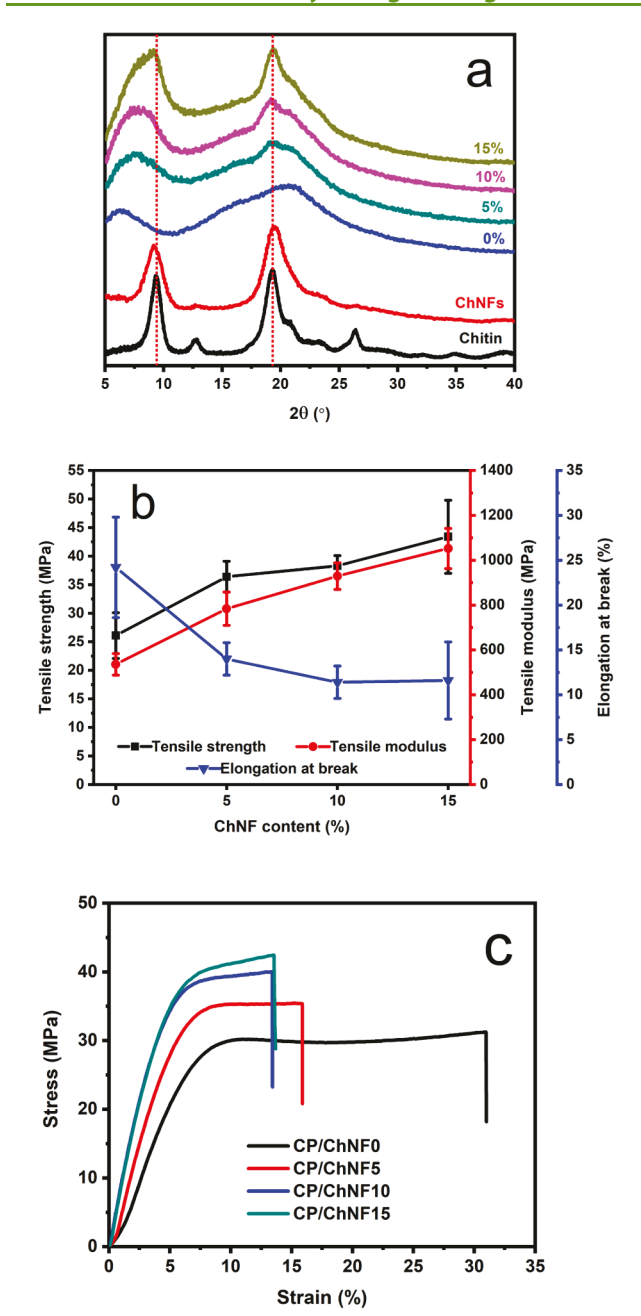


Figure 7. XRD patterns (a) of chitin, ChNFs, and the CP/ChNF nanocomposites with various ChNF contents (0, 5, 10, and 15%); (b) tensile strength, tensile modulus, and the elongation at break and (c) typical stress—strain curves of the series of the nanocomposite films.

Figure 8 shows the temperature-dependent storage modulus and loss tangent tan δ of nanocomposites with various ChNF contents. The storage modulus of the neat CP was reduced smoothly and exhibited glassy modulus with the temperature increased until 150 °C. Above 150 °C, the storage modulus dramatically decreased because of the higher segmental motion of the CP matrix. Another steep reduction in storage modulus happened at around 170 °C, suggesting that the neat CP decomposed before the complete transition from the glassy stage to the rubbery stage. With the increase of ChNF in the CP matrix, the storage modulus was enhanced over a wide range of temperatures. The enhanced storage modulus was observed much more pronounced with increasing ChNF loading at above glass transition temperature $T_{\rm g}$. For example,

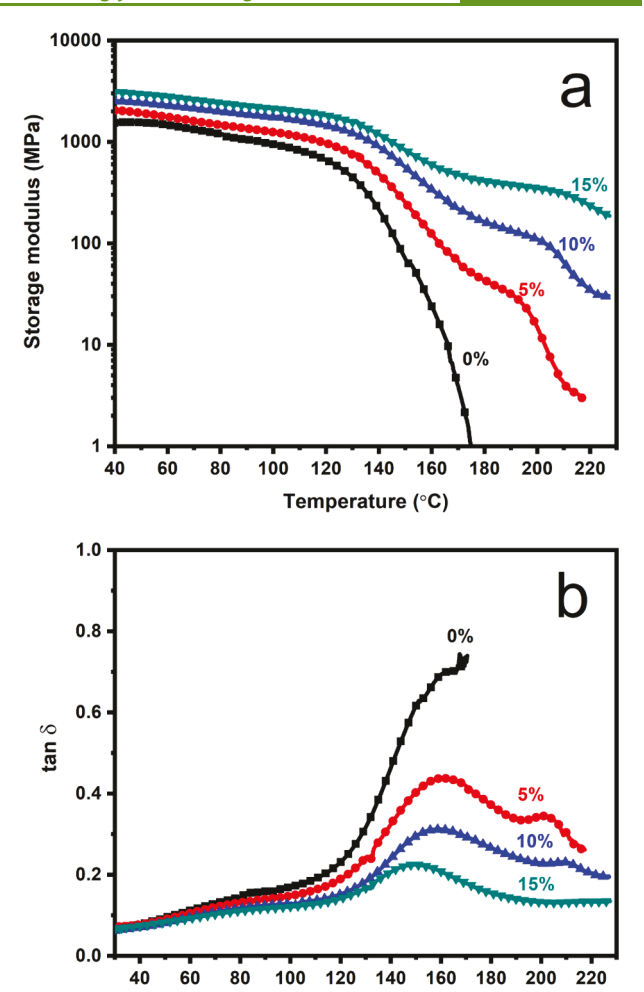


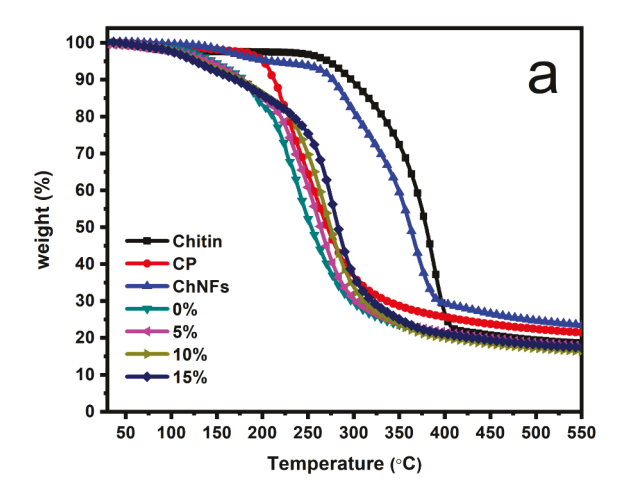
Figure 8. Storage modulus (a) and $\tan \delta$ (b) of the nanocomposites with various ChNF contents (0, 5, 10, and 15%).

Temperature (°C)

the modulus of the nanocomposites containing 15% ChNF at 170 °C was 125 times higher when compared to the neat CP. All the nanocomposites also exhibited a rubbery plateau, which became more evident with higher ChNF addition, indicating the formation of a rigid network and the significant reinforcing effect of ChNF in the matrix. 37,38 Moreover, in contrast to a significant drop in storage modulus of the neat CP at 170 °C, the modulus of the ChNF reinforced CP nanocomposites still maintained a high value up to around 225 °C at the 15% ChNF loading.

Loss tangent ($\tan \delta$) is a measure of the viscoelastic damping of a material. The tan δ peak of the neat CP was not able to be recorded (Figure 8b) due to the quick polymer degradation at around 170 °C. With the ChNF addition, the nanocomposites rendered a complete $\tan \delta$ peak, which decreased in height and was significantly broadened with increased ChNF loading. The results indicated that the nanocomposites became more elastic and could dissipate less during mechanical vibration because CP chain movements might be significantly restrained through nanofibril-matrix interfacial actions and nanofibril-nanofibril interaction including the physical nanofiber network structure at high ChNF loading. 39,40

Thermal Properties of CP/ChNF Nanocomposites. Figure 9 shows the thermal behaviors of the nanocomposites with different ChNF loadings in thermogravimetric analysis



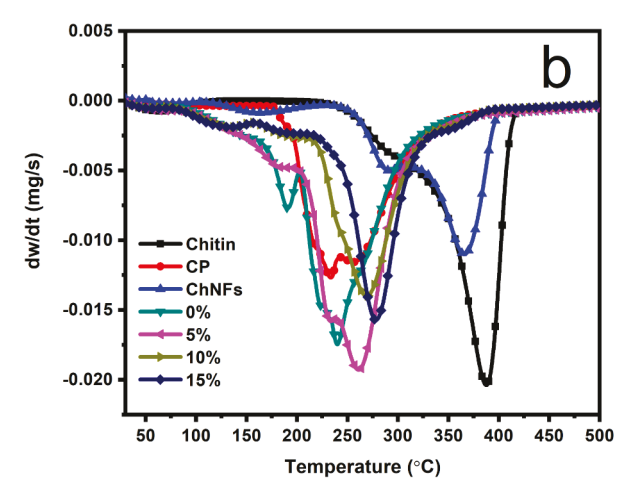


Figure 9. TGA curves (a) and DTG curves (b) of chitin, CP powder, ChNFs, and the nanocomposites with various ChNF contents (0, 5, 10, and 15%).

(TGA) and DTG curves. $T_{\rm max}$ is the peak temperature in DTG curves, which is the degradation temperature linked to the maximum weight loss rate and is often used as an indicator of the thermal stability of a material. The $T_{\rm max}$ for the raw chitin was around 390 °C, which corresponded to the decomposition of the main backbone of the chitin polymer; a shoulder at around 290 °C was attributed to the degradation of the side acetamido groups. The $T_{\rm max}$ for CP powder was around 235 °C with two shoulders around 220 and 260 °C, which might be a result of the degradation of the side groups and the backbone. Comparing the CP film with 0% ChNF to the CP powder, one additional decomposition peak was observed at around 190 °C, which might be ascribed to the decomposition of the low molecular-weight plasticizer. The result indicated that the CP had much lower thermal stability than the raw chitin because well-order molecular chains of chitin often acted as heat barriers and reduced heat diffusion. 42 The propionylation destroyed the crystalline chitin structure, resulting in amorphous CP with less thermal stability. As reported in our previous study, the acylation reaction under the heterogeneous condition in the presence of a strong acid catalyst resulted in much lower intrinsic viscosity than that of raw chitin, indicating a significant decrease in the molecular weight of chitin. This degradation might partly account for a poor thermal stability of propionylated chitin. The $T_{\rm max}$ for the ChNFs was around 365 °C, which was not only slightly lower

than that of the raw chitin but also much higher than that of the CP powder. With the increased ChNF loading in the CP matrix, the thermal degradation temperature of the nanocomposites shifted to higher values. For example, the $T_{\rm max}$ of the 15% ChNF filled nanocomposite was around 280 $^{\circ}{\rm C}$, approximately 40 $^{\circ}{\rm C}$ higher than that of the neat CP film. The thermal stability improvement with ChNF addition in the CP matrix might be largely due to the presence of the crystalline structure and thermal stability of ChNFs.

As noted above, the incorporation of ChNFs in the CP matrix not only improved the film mechanical properties but also significantly enhanced the film's thermal stability, yielding nanocomposite films with good clarity and the partial capability of UV-light shielding. Meanwhile, the CP film containing 15% ChNFs possessed a comparable tensile strength (up to ~43 MPa) to some typical synthetic petroleum-based plastic films such as polyethylene (PE) and polypropylene (PP), and so forth.⁴³ It is long known that traditional PE and PP films play an important role in our ordinary life. However, it was estimated that every year about 8 million tons of these plastics are dumped into the ocean, which need at least several hundred years to be decomposed and pose a threat to marine life. 44 With increasing awareness of the severity of the depletion of fossil fuel sources and "white pollution" that resulted from these nonbiodegradable petroleum-based plastics, more and more academia and industry turned to renewable sources to develop biobased plastics and biodegradable composites. Chitin is a promising renewable source, which was primarily derived from food wastes such as shrimp shells, crab shells, and lobster shells. About 6-8 million tonnes of these decarded shells are generated every year worldwide; waste shells are often just dumped in landfills or the ocean in developing countries while disposal in developed counties can be costly up to 150 dollars per tonne in Australia, for example. With more petroleum-based plastic bans taking effect in different countries globally, these fully chitinderivatized nanocomposite films manufactured from using green acidic ethanol/water processing may be a promising alternative to some synthetic petroleum-based plastic products. These bio-nanocomposite formulations or the resultant films produced in this study may potentially be applied in the fields but not limited to, cosmetics, paintings, coatings, and packaging, and so forth. The use of less toxic or green solvents of processing chitin or chitin derivatives from renewable sources into valued products not only can alleviate the environmental pollution burden to meet sustainability goals but also can create more economic benefits. However, it should be stressed that more material properties, in terms of gas (O₂ and CO₂) barrier properties, water vapor transmission rate, chemical or medium resistance, and so on, still need to be systematically investigated in our future research to validate their applicability to these different fields.

CONCLUSIONS

Chitin-based highly transparent ChNF-reinforced CP nano-composites were developed through using acidified ethanol/water as a medium to dissolve CP and disperse ChNF simultaneously. The ChNF suspension could be directly mixed with CP in the acidified ethanol/water system homogeneously without removing water from the ChNF suspension. Highly transparent solid nanocomposites can be successfully obtained by casting. The ChNF-reinforced CP nanocomposite films had better mechanical properties and thermal stability than the

neat CP, improved by 66% in tensile strength and 97% in tensile modulus at 15% ChNF loading, and by 40 °C in the maximum decomposition temperature, indicating enhanced thermal stability. The storage modulus was higher, and the heat resistance was better than the neat CP over a wide range of temperatures. The significant improvement in mechanical performance and thermal stability might largely be ascribed to the homogeneous distribution of ChNF in CP and good compatibility between the ChNF filler and the CP matrix. The process of dispersing ChNF in the acidified ethanol/water mixture without removing water in ChNF dispersion provides a possible green and facile processing route of direct use of ChNF suspension with other polymers or biopolymers that are soluble in binary ethanol/water mixtures for the development of high-performance ChNF-reinforced nanocomposites.

AUTHOR INFORMATION

Corresponding Authors

Tuhua Zhong — Institute of New Bamboo and Rattan Based Biomaterials, International Center for Bamboo and Rattan, Beijing 100102, China; Composite Materials and Engineering Center, Washington State University, Pullman, Washington 99164, United States; orcid.org/0000-0003-4221-4691; Email: zhongth@icbr.ac.cn

Jinwu Wang — Forest Products Laboratory, U.S. Forest Service, Madison, Wisconsin 53726, United States; orcid.org/0000-0002-8363-1689; Email: jinwu.wang@usda.gov

Authors

Michael P. Wolcott – Composite Materials and Engineering Center, Washington State University, Pullman, Washington 99164, United States; © orcid.org/0000-0003-2733-5559

Hang Liu — Composite Materials and Engineering Center, Washington State University, Pullman, Washington 99164, United States; Apparel, Merchandising, Design, and Textile, Washington State University, Pullman, Washington 99164, United States; orcid.org/0000-0002-8598-9406

Complete contact information is available at: https://pubs.acs.org/10.1021/acssuschemeng.0c08990

Notes

The authors declare no competing financial interest.

■ ACKNOWLEDGMENTS

This work was supported by the Center for Bioplastics and Biocomposites (CB²), a National Science Foundation Industry/University Cooperative Research Center (Awards IIP-1439732 & 1738669).

REFERENCES

- (1) Yan, N.; Chen, X. Don't Waste Seafood Waste. *Nature* 2015, 524, 155–157.
- (2) Kumar, M. N. V. R. A Review of Chitin and Chitosan Applications. *React. Funct. Polym.* **2000**, *46*, 1–27.
- (3) Rinaudo, M. Chitin and Chitosan: Properties and Applications. *Prog. Polym. Sci.* **2006**, 31, 603–632.
- (4) Barber, P. S.; Griggs, C. S.; Bonner, J. R.; Rogers, R. D. Electrospinning of Chitin Nanofibers Directly from an Ionic Liquid Extract of Shrimp Shells. *Green Chem.* **2013**, *15*, 601–607.
- (5) Poirier, M.; Charlet, G. Chitin Fractionation and Characterization in N,N-Dimethylacetamide/Lithium Chloride Solvent System. *Carbohydr. Polym.* **2002**, *50*, 363–370.
- (6) Qin, Y.; Lu, X.; Sun, N.; Rogers, R. D. Dissolution or Extraction of Crustacean Shells Using Ionic Liquids to Obtain High Molecular

Weight Purified Chitin and Direct Production of Chitin Films and Fibers. *Green Chem.* **2010**, *12*, 968–997.

- (7) Edgar, K. J.; Buchanan, C. M.; Debenham, J. S.; Rundquist, P. A.; Seiler, B. D.; Shelton, M. C.; Tindall, D. Advances in Cellulose Ester Performance and Application. *Prog. Polym. Sci.* **2001**, *26*, 1605–1688.
- (8) Kurita, K. Chemistry and Application of Chitin and Chitosan. *Polym. Degrad. Stab.* **1998**, *59*, 117–120.
- (9) Teramoto, Y.; Miyata, T.; Nishio, Y. Dual Mesomorphic Assemblage of Chitin Normal Acylates and Rapid Enthalpy Relaxation of Their Side Chains. *Biomacromolecules* **2006**, *7*, 190–198.
- (10) Hirayama, H.; Yoshida, J.; Yamamoto, K.; Kadokawa, J.-i. Facile Acylation of α -Chitin in Ionic Liquid. *Carbohydr. Polym.* **2018**, 200, 567–571.
- (11) Draczynski, Z. Synthesis and Solubility Properties of Chitin Acetate/Butyrate Copolymers. *J. Appl. Polym. Sci.* **2011**, 122, 175–182.
- (12) Yang, B. Y.; Ding, Q.; Montgomery, R. Preparation and Physical Properties of Chitin Fatty Acids Esters. *Carbohydr. Res.* **2009**, 344, 336–342.
- (13) Alexandre, M.; Dubois, P. Polymer-Layered Silicate Nano-composites: Preparation, Properties and Uses of a New Class of Materials. *Mater. Sci. Eng.*, R 2000, 28, 1–63.
- (14) Dufresne, A. Cellulose Nanomaterial Reinforced Polymer Nanocomposites. *Curr. Opin. Colloid Interface Sci.* **2017**, *29*, 1–8.
- (15) Ifuku, S.; Saimoto, H. Chitin Nanofibers: Preparations, Modifications, and Applications. *Nanoscale* **2012**, *4*, 3308–3318.
- (16) Goodrich, J. D.; Winter, W. T. α -Chitin Nanocrystals Prepared from Shrimp Shells and Their Specific Properties. *Biomacromolecules* **2007**, *8*, 252–257.
- (17) Fan, Y.; Saito, T.; Isogai, A. Chitin Nanocrystals Prepared by TEMPO-Mediated Oxidation of α -Chitin. *Biomacromolecules* **2008**, *9*, 192–198.
- (18) Fan, Y.; Saito, T.; Isogai, A. Individual Chitin Nano-Whiskers Prepared From Partially Deacetylated α -Chitin by Fibril Surface Cationization. *Carbohydr. Polym.* **2010**, *79*, 1046–1051.
- (19) Peng, Y.; Gardner, D. J.; Han, Y. Drying Cellulose Nanofibrils: In Search of a Suitable Method. *Cellulose* **2012**, *19*, 91–102.
- (20) Ifuku, S.; Ikuta, A.; Egusa, M.; Kaminaka, H.; Izawa, H.; Morimoto, M.; Saimoto, H. Preparation of High-Strength Transparent Chitosan Film Reinforced with Surface-Deacetylated Chitin Nanofibers. *Carbohydr. Polym.* **2013**, *98*, 1198–1202.
- (21) Zhong, T.; Wolcott, M. P.; Liu, H.; Wang, J. Developing Chitin Nanocrystals for Flexible Packaging Coatings. *Carbohydr. Polym.* **2019**, 226, 115276.
- (22) Wang, T.; Drzal, L. T. Cellulose-Nanofiber-Reinforced Poly(Lactic Acid) Composites Prepared by a Water-Based Approach. ACS Appl. Mater. Interfaces 2012, 4, 5079–5085.
- (23) Tang, L.; Weder, C. Cellulose Whisker/Epoxy Resin Nanocomposites. ACS Appl. Mater. Interfaces 2010, 2, 1073–1080.
- (24) Zhong, T.; Wolcott, M. P.; Liu, H.; Wang, J. Propionylation-Modified Chitin with Improved Solubility in Green Ethanol/Water Binary Solvents for Sustainable Film and Coating Applications. *J. Clean. Prod.* **2020**, 250, 119458.
- (25) Brugnerotto, J.; Lizardi, J.; Goycoolea, F. M.; Argüelles-Monal, W.; Desbrières, J.; Rinaudo, M. An Infrared Investigation in Relation with Chitin and Chitosan Characterization. *Polymer* **2001**, *42*, 3569–3580.
- (26) Sabnis, S.; Block, L. H. Improved Infrared Spectroscopic Method for the Analysis of Degree of N-Deacetylation of Chitosan. *Polym. Bull.* **1997**, *39*, 67–71.
- (27) Cárdenas, G.; Cabrera, G.; Taboada, E.; Miranda, S. P. Chitin Characterization by SEM, FTIR, XRD, and 13C Cross Polarization/ Mass Angle Spinning NMR. *J. Appl. Polym. Sci.* **2004**, 93, 1876–1885.
- (28) Hoogenboom, R.; Rogers, S.; Can, A.; Becer, C. R.; Guerrero-Sanchez, C.; Wouters, D.; Hoeppener, S.; Schubert, U. S. Self-Assembly of Double Hydrophobic Block Copolymers in Water-Ethanol Mixtures: From Micelles to Thermoresponsive Micellar Gels. *Chem. Commun.* **2009**, *37*, 5582–5584.

- (29) Zhang, Q.; Schattling, P.; Theato, P.; Hoogenboom, R. Tuning the Upper Critical Solution Temperature Behavior of Poly(Methyl Methacrylate) in Aqueous Ethanol by Modification of an Activated Ester Comonomer. *Polym. Chem.* **2012**, *3*, 1418–1426.
- (30) Zhang, Q.; Hoogenboom, R. Polymers with Upper Critical Solution Temperature Behavior in Alcohol/Water Solvent Mixtures. *Prog. Polym. Sci.* **2015**, *48*, 122–142.
- (31) Ifuku, S.; Morooka, S.; Norio Nakagaito, A.; Morimoto, M.; Saimoto, H. Preparation and Characterization of Optically Transparent Chitin Nanofiber/(Meth)Acrylic Resin Composites. *Green Chem.* **2011**, *13*, 1708–1711.
- (32) Duan, B.; Chang, C.; Ding, B.; Cai, J.; Xu, M.; Feng, S.; Ren, J.; Shi, X.; Du, Y.; Zhang, L. High Strength Films with Gas-Barrier Fabricated from Chitin Solution Dissolved at Low Temperature. *J. Mater. Chem. A* **2013**, *1*, 1867–1874.
- (33) Iwatake, A.; Nogi, M.; Yano, H. Cellulose Nanofiber-Reinforced Polylactic Acid. *Compos. Sci. Technol.* **2008**, *68*, 2103–2106
- (34) Fujisawa, S.; Okita, Y.; Fukuzumi, H.; Saito, T.; Isogai, A. Preparation and Characterization of TEMPO-Oxidized Cellulose Nanofibril Films with Free Carboxyl Groups. *Carbohydr. Polym.* **2011**, *84*, 579–583.
- (35) Liu, D.; Sun, X.; Tian, H.; Maiti, S.; Ma, Z. Effects of Cellulose Nanofibrils on the Structure and Properties on PVA Nanocomposites. *Cellulose* **2013**, *20*, 2981–2989.
- (36) Soeta, H.; Fujisawa, S.; Saito, T.; Berglund, L.; Isogai, A. Low-Birefringent and Highly Tough Nanocellulose-Reinforced Cellulose Triacetate. *ACS Appl. Mater. Interfaces* **2015**, *7*, 11041–11046.
- (37) Song, L.; Wang, Z.; Lamm, M. E.; Yuan, L.; Tang, C. Supramolecular Polymer Nanocomposites Derived from Plant Oils and Cellulose Nanocrystals. *Macromolecules* **2017**, *50*, 7475–7483.
- (38) Yue, L.; Maiorana, A.; Khelifa, F.; Patel, A.; Raquez, J.-M.; Bonnaud, L.; Gross, R.; Dubois, P.; Manas-Zloczower, I. Surface-Modified Cellulose Nanocrystals for Biobased Epoxy Nanocomposites. *Polymer* **2018**, *134*, 155–162.
- (39) Xu, X.; Liu, F.; Jiang, L.; Zhu, J. Y.; Haagenson, D.; Wiesenborn, D. P. Cellulose Nanocrystals vs. Cellulose Nanofibrils: A Comparative Study on Their Microstructures and Effects as Polymer Reinforcing Agents. ACS Appl. Mater. Interfaces 2013, 5, 2999–3009.
- (40) Grunert, M.; Winter, W. T. Nanocomposites of Cellulose Acetate Butyrate Reinforced with Cellulose Nanocrystals. *J. Polym. Environ.* **2002**, *10*, 27–30.
- (41) Kumar, N. A.; Rejinold, N. S.; Anjali, P.; Balakrishnan, A.; Biswas, R.; Jayakumar, R. Preparation of Chitin Nanogels Containing Nickel Nanoparticles. *Carbohydr. Polym.* **2013**, *97*, 469–474.
- (42) Morgado, D. L.; Frollini, E. Thermal Decomposition of Mercerized Linter Cellulose and Its Acetates Obtained from a Homogeneous Reaction. *Polimeros* **2011**, *21*, 111–117.
- (43) Raab, M.; Kotulák, L.; Kolařík, J.; Pospíšil, J. The Effect of Ultraviolet Light on the Mechanical Properties of Polyethylene and Polypropylene Films. *J. Appl. Polym. Sci.* **1982**, *27*, 2457–2466.
- (44) Liu, C.; Luan, P.; Li, Q.; Cheng, Z.; Sun, X.; Cao, D.; Zhu, H. Biodegradable, Hygienic, and Compostable Tableware from Hybrid Sugarcane and Bamboo Fibers as Plastic Alternative. *Matter* **2020**, *3*, 2066–2079.